Mangels, J.A., Ivry, R.B., Shimizu, N., 1998. Dissociable contributions of the prefrontal and neocerebellar cortex to time perception. Brain Res. Cogn. Brain Res. 7, 15–39.
Maquet, P., Peters, J., Peters, J., Aerts, J., Delfiore, G., Degueldre, C., Luxen, A., Franck, G., 1996. Functional neuroanatomy of human rapid-eye-movement sleep and dreaming. Nature 383, 163–166.
Maquet, P., Degueldre, C., Delfiore, G., Aerts, J., Peters, J.M., Luxen, A., Franck, G., 1997. Functional neuroanatomy of human slow wave sleep. J. Neurosci. 17, 2807–2812.
Maquet, P., 2000. Functional neuroimaging of normal human sleep by positron emission tomography. J. Sleep Res. 9, 207–231.
Moiseeva, N.I., 1975. The characteristics of EEG activity and the subjective estimation of time during dreams of different structure. Electroencephalogr. Clin. Neurophysiol. 38, 569–577.
Moorcroft, W.H., Kayser, K.H., Griggs, A.J., 1997. Subjective and objective confirmation of the ability to self-awaken at a self-predetermined time without using external means. Sleep 20, 40–45.
Morell, V., 1996. Setting a biological stopwatch. Science 271, 905–906.
Omwake, K.T., Loranz, M., 1933. Study of ability to wake at a specified time. J. Appl. Psychol., 468–474.
Perlis, M.L., Giles, D.E., Mendelson, W.B., Bootzin, R.R., Wyatt, J.K., 1997. Psychophysiological insomnia: the behavioural model and a neurocognitive perspective. J. Sleep Res. 6, 179–188.
Rao, S.M., Mayer, A.R., Harrington, D.L., 2001. The evolution of brain activation during temporal processing. Nat. Neurosci. 4, 317–323.
Rechtschaffen, A., Kales, A., 1968. A Manual of Standardized Terminology, Techniques and Scoring System for Sleep Stages of Human Subjects.
Salin-Pascual, R.J., Roehrs, T.A., Merlotti, L.A., Zorick, F., Roth, T., 1992. Long-term study of the sleep of insomnia patients with sleep state misperception and other insomnia patients. Am. J. Psychiatry. 149, 904–908.
Shibui, K., Uchiyama, M., Okawa, M., Kudo, Y., Kim, K., Liu, X., Kamei, Y., Hayakawa, T., Akamatsu, T., Ohta, K., Ishibashi, K., 2000. Diurnal fluctuation of sleep propensity and hormonal secretion across the menstrual cycle. Biol. Psychiatry 48, 1062–1068.
Spati, J., Munch, M., Blatter, K., Knoblauch, V., Jones, L.A., Cajochen, C., 2009. Impact of age, sleep pressure and circadian phase on time-of-day estimates. Behav. Brain Res. 201, 48–52.
Tang, N.K., Harvey, A.G., 2005. Time estimation ability and distorted perception of sleep in insomnia. Behav. Sleep Med. 3, 134–150.
Tart, C.T., 1970. Waking from sleep at a preselected time. J. Am. Soc. Psychosom. Dent. Med. 17, 3–16.
Vanable, P.A., Aikens, J.E., Tadimeti, L., Caruana-Montaldo, B., Mendelson, W.B., 2000. Sleep latency and duration estimates among sleep disorder patients: variability as a function of sleep disorder diagnosis, sleep history, and psychological characteristics. Sleep 23, 71–79.
Weber, J., Schwander, J.C., Unger, I., Meier, D., 1997. A direct ultrasensitive RIA for the determination of melatonin in human saliva: comparison with serum levels. Sleep Res. 26, 757.
Zepelin, H., 1986. REM sleep and the timing of self-awakenings. Bull. Psychom. Soc. 24, 254–256.
Zung, W.W., Wilson, W.P., 1971. Time estimation during sleep. Biol. Psychiatry. 3, 159–164.

J Med Dent Sci 2010; 57: 185–192

Original Article

Ultrasonic anisotropy measured in 2-dimensional echocardiograms in vitro and verified by histology

Junko Komata[1], Tokuhiro Kawara[1], Kazuyoshi Tanaka[1], Sera Hirota[1], Sayaka Nishi[1], Yuichiro Cho[2], Kenji Sato[2], Masato Matsuura[1] and Itsuro Miyazato[1]

1) Department of Biofunctional Informatics, Graduate School of Health Care Sciences, Tokyo Medical and Dental University
2) Department of Anatomy and Physiological Science, Graduate School of Health Care Sciences, Tokyo Medical and Dental University

This study aims to validate ultrasonic anisotropy in 2-dimensional echocardiograms by one-to-one histological correlation. Thirteen echograms were obtained in vitro from 9 specimens of 2 left ventricles of healthy adult beagle dogs and were correlated with corresponding histology in regard to ultrasound orientation relative to the local fiber direction. Median value of pixel echogenicity (255-rank) was lower in areas with parallel (n = 9, 18 ± 13) than in those with oblique (n = 7, 41 ± 14, $P < 0.05$) and perpendicular (n = 13, 57 ± 21, $P < 0.01$) ultrasound orientations. Echogenicity in the proximal part within 0.5 cm from an edge was relatively high (n = 9, 33 ± 15; n = 5, 66 ± 27; n = 8, 65 ± 32, respectively) and was different between parallel and perpendicular orientations ($P < 0.05$). The ratio of the distal adjacent 0.5-cm part to the proximal part echogenicity was lower for either parallel or oblique orientation (0.35 ± 0.25, 0.51 ± 0.16) than for perpendicular orientation (0.95 ± 0.16, $P < 0.01$, respectively). Acoustic dropouts appeared beyond myocardial areas with parallel or oblique ultrasound orientation. These results disclosed precise acoustic anisotropy in the 2-dimensional echocardiograms.

Corresponding Author: Tokuhiro Kawara
Department of Biofunctional Informatics, Graduate School of Health Care Sciences, Tokyo Medical and Dental University, 1-5-45, Yushima, Bunko-ku, Tokyo 113-8519, Japan
Tel: +81-3-5803-5365 Fax: +81-3-5803-5365
E-mail: tkawara.mtec@tmd.ac.jp
Received April 15 ; Accepted June 11, 2010

Key words: Echocardiography, Myocardium, Ultrasound

Introduction

Ultrasonic anisotropy has been measured in amplitude mode with animal myocardium[1-3], and normal or diseased human myocardium[4-7]. Backscatter is small and attenuation is great if ultrasound propagates at a parallel angle relative to the local fiber direction, and vice versa if it propagates at a perpendicular angle[1-7]. There is an inherent myocardial architecture[8,9]: diagonal or longitudinal on the outside, circular in the mid-area, and oppositely diagonal or longitudinal in the inside layer of the left ventricle. Ultrasound orientation relative to local fiber direction is attributed to commonly observed echogenic patterns in clinical echocardiograms[10,11]. For instance, in the short axis view, the inferior septum and anterior wall appear dark and sometimes make acoustic dropouts, while in the same view, the anterior septum and posterior wall appear bright; moreover, in the apical four-chamber view, the interventricular septum looks 3-layered, bright in the mid-area and dark at both borders. Under these circumstances, it is reasonably speculated that the local myocardial fiber direction may be estimated from corresponding echocardiogram on the basis of ultrasonic anisotropy at least in part. Meanwhile, ultrasonic anisotropy has been extensively reported using amplitude-mode[1,3,7] or M-mode[2] with specifically designed apparatuses, but insensibly using 2-dimensional mode with a clinical imager[12]. Furthermore, the lack of direct correlation between 2-dimensional echogram and histology of the identical myocardium prevents us from realizing the impact and way of ultrasonic anisotropy in clinical echocardiograms. The

purpose of this study was to correlate 2-dimensional echograms and histology from the same planes of healthy canine left ventricles in a one-to-one manner, demonstrating how these correspond to each other in regard to ultrasound versus fiber orientation.

Materials and methods

Myocardial specimens

Two adult beagle dogs underwent thoracotomy and stimulation tests of the sympathetic nervous trunk and were sacrificed with a lethal amount of pentobarbital with permission of the local ethics committee of animal experiments. Hearts were then excised, immediately immersed and rinsed in cold saline, and then 9 myocardial specimens about 1 cm thick were carved out. One heart yielded basal anterior and posterior walls, basal anterior and inferior septum in the basal short axis plane, and anterolateral papillary muscle with corresponding ventricular wall. The other heart yielded mid-septum and lateral wall, and apical septum and lateral wall in the apical four-chamber plane.

Image acquisition

Fresh myocardial specimens were examined for echography in a cold-saline-filled bath while taking extreme care concerning bubbling. The whole inner surface of the bath was covered with sheets of wrinkled aluminum foil to avoid ultrasound resonance. Echograms were obtained with an echograph Voyager (Ardent Sound, Mesa, AZ, U.S.A.) and a 10-MHz mechanical scanning transducer. The gel-immersed head of the transducer was wrapped with thermoplastic and tied to a column support, and then inserted into the saline. The myocardial specimens were pinned to a rubber plug, which was magnetically fitted to the inner surface of the bath at a distance of 0.5 to 2.5 cm from the transducer head. Specimens from the interventricular septum and left ventricular wall were set and scanned as in the basal short axis view or apical four-chamber view. The papillary muscle was scanned in a plane parallel to the epicardium in 5 directions: from base, anterior, posterior, basal anterior, and basal posterior oriented as in vivo. In addition, echograms were taken from some of the myocardial specimens with pinheads to ascertain the acoustic dropout from the myocardium and its dependence on ultrasound orientation. Echo gain and sensitivity time controllers were adjusted initially and set constant for the total examinations. Digital frames were stored as BMP image files and analyzed later.

Histology

From the 9 myocardial specimens after formalin fixation, slices in the respective echographic planes with a 10-μm thickness were cut. The slices were stained with Masson's trichrome (turns cytoplasm red and collagen blue) and examined by light microscopy. Regions with an approximately uniform fiber direction were scoped in each slice.

Echogenicity

Echogenicity of areas corresponding to uniformly-fiber-directed myocardial regions were determined using a 255-rank histogram construction function of image-editing software Photoshop Elements 7 (Adobe Systems, San Jose, CA, USA) , which gave interval scale data of brightness for pixels in selected areas of echograms. The leading edges of the myocardial images were excluded from the analysis. The median echogenicity value of the corresponding pixels was adopted as representative for each area. Ultrasound orientation was determined as parallel, perpendicular or oblique relative to the local fiber direction in each area and echogenicity was compared among those with different ultrasound orientations.

If ultrasound initially propagated a 1-cm or longer uniformly-fiber-directed myocardial region, echogenicity as a function of distance was evaluated. Echogenicity in the sequential proximal and distal parts with a respective length of 0.5 cm beginning from the near end of the myocardial image was measured, and the ratio of distal to proximal part echogenicity was calculated. Echogenicity of the proximal part and the ratio of distal to proximal part echogenicity were compared among areas with different ultrasound orientations relative to fiber direction.

Statistical analysis

Numerical data were expressed as mean $\pm$ SD after verification of normality and homoscedasticity by chi-square test for goodness of fit and Bartlett test, respectively. Thereafter, one-way analysis of variance and Tukey's test were performed. All analyses were performed using Excel 2007 (Microsoft, Redmond, WA, USA) add-in software Ekuseru-Toukei 2008 for Windows version 1.07 (Social Survey Research Information, Tokyo, Japan), and $P < 0.05$ was considered statistically significant.

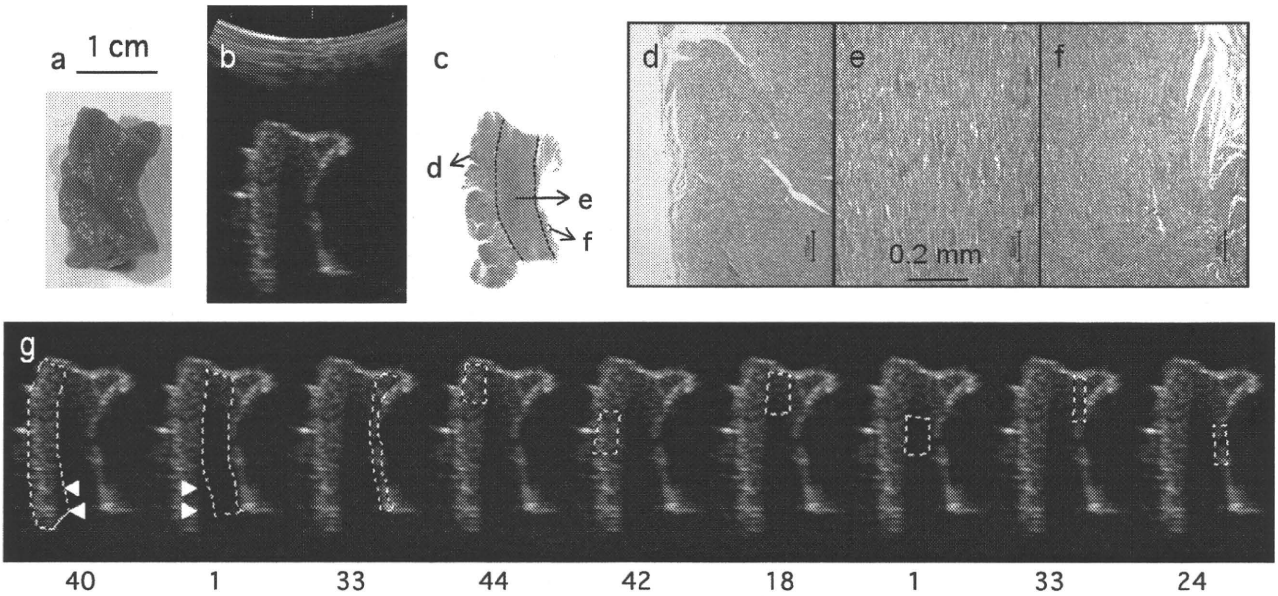

Figure 1 : Results from the basal posterior septum in a short axis plane. **a** Picture showing the specimen with the left ventricular endocardium on the right. **b** Echographic image scanned from the anterior. **c** Slice stained with Masson's trichrome showing red cytoplasm and blue collagen, with dashed lines indicating borders of 3 uniformly-fiber-directed regions. **d, e, f** Microscopic images from the small boxes indicated in **c** showing transverse (d), vertical lengthwise (e), and vertical short lengthwise (f) myocytes, meaning respective perpendicular, parallel, and oblique ultrasound orientations relative to the fiber direction. **g** Areas corresponding to uniformly-fiber-directed region (left 3 panels) and proximal and distal parts (right 6 panels) indicated with dashed lines and respective echogenicity values (255-rank) below. The lower inner-hand margin of the right ventricular subendocardial area (open triangles) seemed under acoustic dropout by the upper mid-region.

Results

Fiber direction and ultrasound orientation relative to fiber direction

Three main regions of uniform fiber direction were observed in the respective myocardial specimens, except for the papillary muscle showing an almost uniformly longitudinal fiber direction. Transitions of the fiber directions between the adjacent main regions were abrupt in some locations and gradual in others. Widths of the regions were not always equal. Borders of regions were occasionally indented. The specimens showed a predominant pattern of fiber direction, namely, circular in the mid-layer and longitudinal both in the outside and inside layers except for the basal posterior wall and two apical regions. The basal posterior wall showed diagonal and spiral fiber directions in the mid-layer and circular fiber direction in the subepicardial layer. The left subendocardial layer of the apical septum and the subepicardial layer of the apical lateral wall showed diagonal fiber direction. Totally, the ultrasonic beam was oriented parallel, oblique and perpendicular to the local fiber direction in 9, 7 and 13 areas, respectively. Ultrasound initially propagated 1-cm or longer uniformly-fiber-directed myocardial regions with 9 parallel, 5 oblique, and 8 perpendicular orientations to the local fiber direction, respectively.

Correlation between echograms and histology

Twenty-five uniformly-fiber-directed regions in the 9 slices were correlated with 29 corresponding areas in 13 echograms.

Figure 1 shows the results from a basal inferior septum specimen in a short axis plane. Myocytes in the right ventricular subendocardial region appeared with transverse sections, those in the mid-region with vertical lengthwise sections, and those in the thin left ventricular subendocardial region with vertical but short lengthwise sections in histology, meaning perpendicular, parallel and oblique ultrasound orientations relative to the local fiber direction in the respective regions. Echogenicity (255-rank) was very low in the mid-area (1) in comparison to the right and left ventricular subendocardial areas (40, 33). This difference was

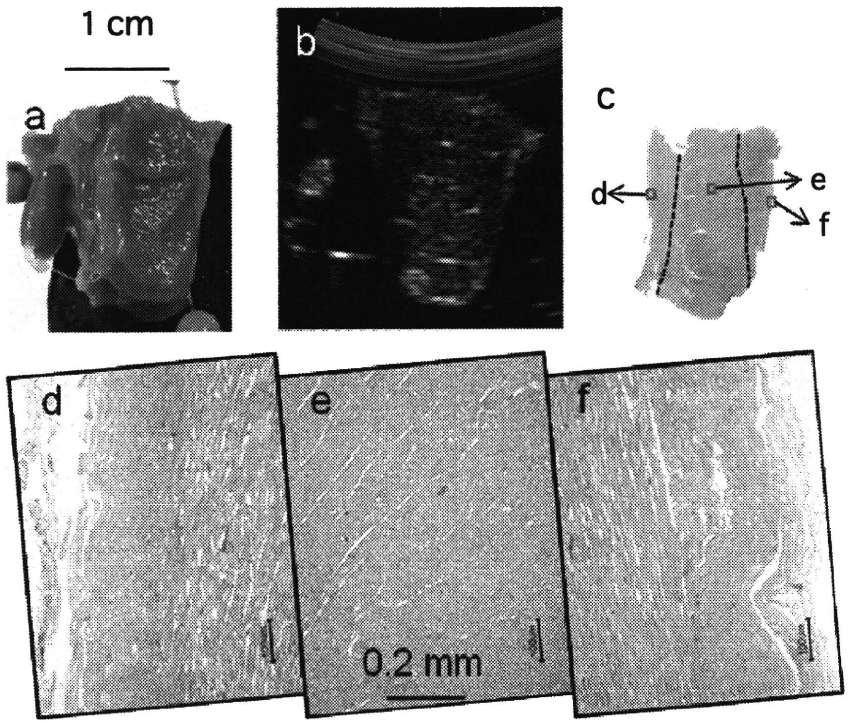

Figure 2 : Results from the mid-septum in an apical four-chamber plane. **a** Picture showing the specimen with the left ventricular endocardium on the right. **b** Echographic image scanned from apex. **c** Slice stained with Masson's trichrome with dashed lines indicating borders of 3 uniformly-fiber-directed regions. **d, e, f** Microscopic images from the small boxes indicated in **c** showing vertical lengthwise (d, f), and transverse (e) myocytes, meaning respective parallel and perpendicular ultrasound orientations relative to the fiber direction.

small in the proximal parts (18 vs. 44 and 33). The ratio of distal to proximal part echogenicity was low in the mid-area (0.06), high in the right ventricular subendocardial area (0.95), and intermediate in the left ventricular subendocardial area (0.73). There seemed an acoustic dropout in the lower mid-area beginning at less than 1 cm from the near end of the myocardial image that eclipsed the lower inner side of the right ventricular subendocardial region (Figure 1g, left two panels).

Figure 2 shows the results from a mid-septum specimen in an apical four-chamber plane. Myocytes in the right and left ventricular subendocardial regions appeared with vertical lengthwise sections, and those in the mid-region with transverse sections, meaning parallel and perpendicular ultrasound orientations relative to the local fiber direction in the respective regions. Echogenicity was low in the right and left ventricular subendocardial areas (14, 26) in comparison to the mid-area (39). This difference was small in the proximal parts (21 and 29 vs. 32). The ratio of distal to proximal part echogenicity was low in the right and left ventricular subendocardial areas (0.43, 0.69) in comparison to the mid-area (0.97). Here again, there seemed an acoustic dropout in the lower right ventricular subendocardial region beginning at less than 1 cm from the incident site.

The results from a papillary muscle specimen are shown partly in Figure 3. Myocytes in the papillary muscle appeared with vertical lengthwise sections. Ultrasound orientation relative to the local fiber direction was parallel with scanning from base, perpendicular with scanning from anterior and posterior, and oblique with scanning from basal anterior and basal posterior, respectively. The obvious speckle pattern in the papillary muscle area was always directed orthogonal to the ultrasonic beam and independent from the local fiber direction. Echogenicity in the papillary muscle area was low with scanning from base (3), high with scanning from anterior and posterior (83, 97), and intermediate with scanning from basal anterior and basal posterior (57, 46). This difference

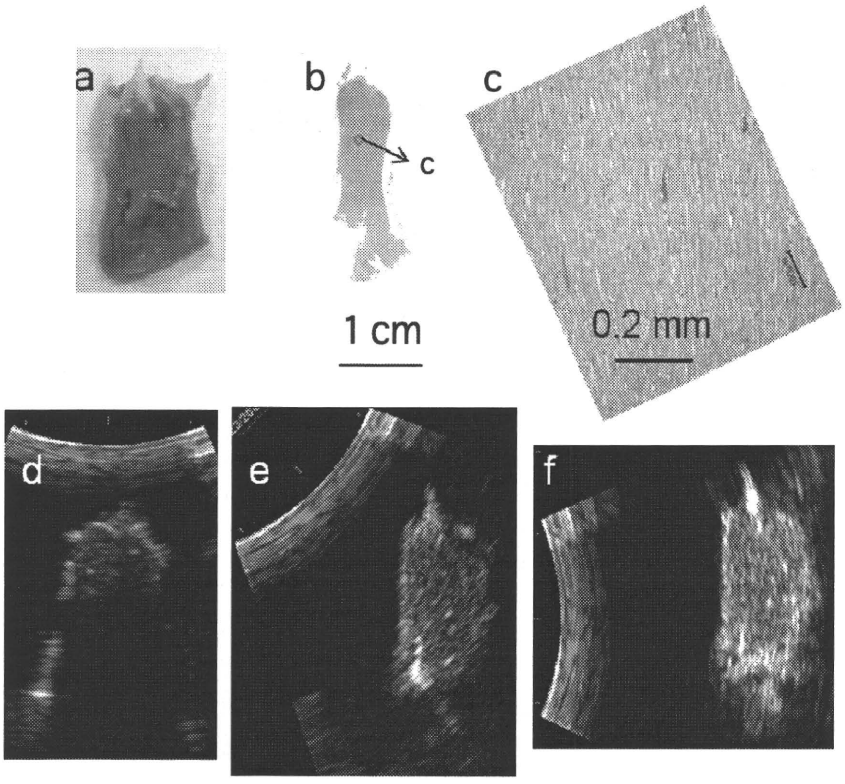

Figure 3 : Results from the papillary muscle in a plane parallel to the epicardium. **a** Picture showing the specimen with the vertex at the top. **b** Slice stained with Masson's trichrome. **c** Microscopic image from the small box indicated in **b** showing vertical lengthwise myocytes. **d, e, f** Echographic images scanned from base (d), basal posterior (e), and posterior (f), under parallel, oblique, and perpendicular ultrasound orientations relative to the local fiber direction, respectively.

was small in the proximal parts (base, 37; anterior, 90; posterior, 95; basal anterior, 89; basal posterior, 63). The ratio of distal to proximal part echogenicity was low with scanning from base (0.08), high with scanning from anterior and posterior (0.84, 1.09), and intermediate with scanning from basal anterior and basal posterior (0.43, 0.59). An acoustic dropout appeared beyond 0.5 to 1 cm from the incident site by scanning from base (Figure 3d).

Taken together, echogenicity was lower in areas with parallel ultrasound orientation than in those with oblique and perpendicular orientations relative to the local fiber direction (18 ± 13 vs. 41 ± 14, 57 ± 21; $P < 0.05$, $P < 0.01$, respectively). Proximal part echogenicity was relatively high (parallel, 33 ± 15; oblique, 66 ± 27; perpendicular, 65 ± 32), and the difference was significant only between areas with parallel and perpendicular ultrasound orientations ($P < 0.05$). The ratio of distal to proximal part echogenicity was lower in areas with parallel and oblique orientations (0.35 ± 0.25, 0.51 ± 0.16) than in areas with perpendicular orientation (0.95 ± 0.16) ($P < 0.01$, respectively).

Acoustic dropout by myocardium

The acoustic dropouts were typically demonstrated by some of the myocardial specimens under parallel or oblique ultrasound orientation relative to the local fiber direction (Figure 4, 5). The slice of the basal anterior wall in a short axis plane revealed myocytes with transverse sections in the subendocardial region, vertical lengthwise sections in the mid-region, and vertical short lengthwise sections in the subepicardial region, meaning perpendicular, parallel, and oblique ultrasound orientations, respectively. When a pinhead was located below the subendocardial region, it made a strong and largely reverberated echo signal (Figure 4a). However, the pinhead made a weak and only slightly reverberated echo signal when it was located below the mid-region (Figure 4b), and a fragmentary echo

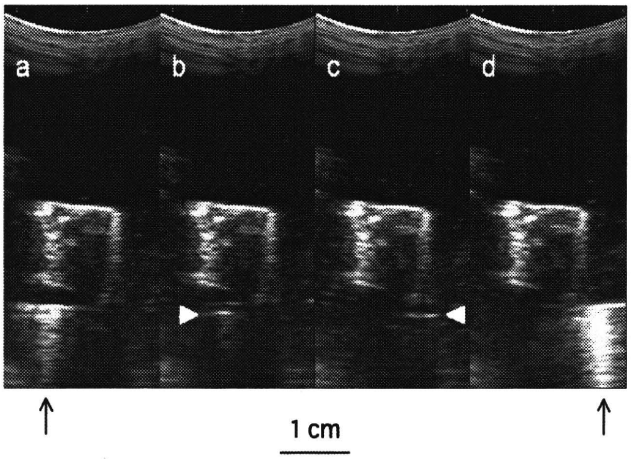

Figure 4 : Acoustic dropout made by the basal anterior wall in a short axis plane. **a, b, c, d** Echograms scanned from the anterior showing scarce (b, triangle) and fragmentary (c, triangle) images of pinheads below the mid- and subepicardial regions respectively despite apparent and strongly reverberated images of those below the endocardial (a, arrow) and just outside and below the epicardial (d, arrow) regions.

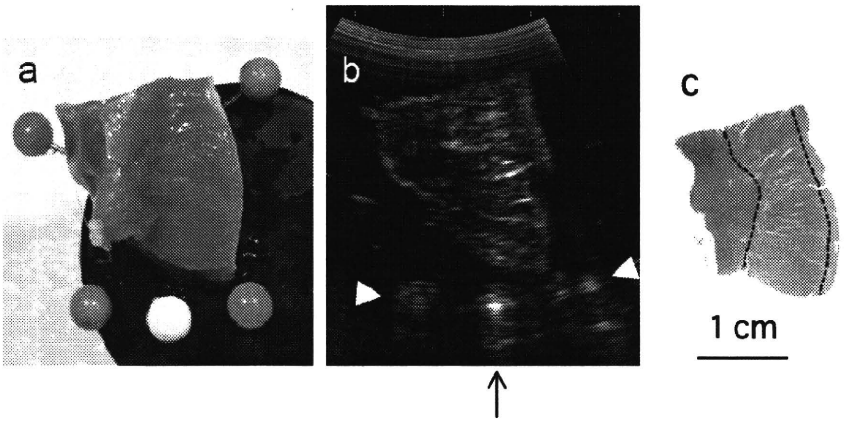

Figure 5 : Acoustic dropout made by the mid-lateral wall in an apical four-chamber plane. **a** Picture showing the specimen with the endocardium on the left and 3 pinheads in the same plane below. **b** Echogram from apex showing a subtle (left triangle) and deficient (right triangle) images of pinheads below the respective subendocardial and subepicardial regions despite an apparent and highly reverberated image of that below the mid-region (arrow). **c** Slice stained with Masson's trichrome with dashed lines indicating borders of 3 uniformly-fiber-directed regions; vertical in both subendocardial and thin subepicardial regions and normal in the mid-region, meaning parallel and perpendicular ultrasound orientations in the respective areas.

signal when located below the subepicardial region (Figure 4c). Finally, when the pinhead was located just outside and below the epicardial region, it made a very strong and highly reverberated echo signal again (Figure 4d). The slice of the mid-lateral wall in an apical four-chamber plane revealed myocytes with transverse sections in the mid-region, with vertical lengthwise sections both in the subendocardial and thin subepicardial regions, meaning perpendicular and parallel ultrasound orientations, respectively (Figure 5C). A pinhead below the mid-region generated a hyperechoic reverberated image. However, that below the subendocardial region generated a subtle echo image and that below the subepicardial region a deficient echo image (Figure 5a, 5b).

Discussion

The 2-dimensional echograms and histology in the identical planes of canine hearts were closely correlated in this study. The variance of echogenicity was fairly explained by the ultrasound orientation relative to local fiber direction. Echogenicity was low in areas with parallel ultrasound orientation in comparison to those with oblique or perpendicular orientation.

Another similar study using a clinical imager treated the interventricular septum and lateral wall in the apical four-chamber view and relied on the intrinsic myocardial fiber direction[12]. Regional variations in our study, however, required microscopic inspection for each region both for precise locations of the uniformly-fiber-oriented region and for discriminations of the oblique fiber direction from either longitudinal or transverse fiber direction. The results disclosed regional precision of correlation between 2-dimensional echograms and histology in regard to ultrasound versus fiber orientation.

Acoustic dropout appeared 0.5 to 1 cm beyond ultrasound propagation parallel or oblique to the local fiber direction even if the uniformly-fiber-directed region was as wide as several mm. Accordingly, myocardial regions arrayed nearly parallel to the ultrasonic beam could be well highlighted by acoustic dropouts in clinical echocardiograms, with accuracy in location and width. This could be a unique key to evaluate myocardial fiber architecture by echocardiography.

Myocardial ultrasonic anisotropy was observed pronouncedly in distal areas from the ultrasonic incident site, which supports attenuation as a main cause of ultrasonic anisotropy[3,7,12]. The specific myocardial area is propagated with minor ultrasound because of attenuation from passing along the fibers, and it finally becomes out of ultrasound reach. In contrast to acoustic shadow generating echo dropout beyond strong echo by reflection of most ultrasound energy, attenuation generates gradual echo dropout by the medium itself, which is misleading in clinical echocardiograms.

Myocardial ultrasonic anisotropy was observed even in areas very proximal to the ultrasonic incident site, which may suggest reflection as a cause of ultrasonic anisotropy in part. Reflection at a border between myocytes and interstitium may favorably return ultrasound energy to the probe, with ultrasound passing across fibers but not along them. In addition, borders between myocytes and interstitium for a certain distance should abound with ultrasound passing across fibers and not along them.

This study focused on regional correlation but not on the exact attenuation rate in acoustic anisotropy. We measured and calculated the ratio of distal to proximal part echogenicity for a distance of 0.5 cm, which was distributed from 0.3 to 0.9, low in the parallel, high in the perpendicular, and intermediate in the oblique ultrasound propagations. In addition, ultrasound orientation relative to the local fiber direction was determined qualitatively. The results could not be compared with attenuation coefficients[3,7,12] as a function of relative angle[3,7] reported in other studies. However, the results were consistent in regard to acoustic anisotropy.

The results were obtained from in vitro experiments. In vivo echocardiograms are affected by other factors, such as subcutaneous fat, ribs, lung, myocardial contraction[2], and so on. In addition, the ultrasonic frequency used in this study was higher than in clinical echocardiography. Therefore, the results of this study cannot be applied directly to clinical echocardiography.

Nonetheless, acoustic dropout originating in a myocardial area due to attenuation with an adjacent hyperechoic region from qualitative observation can be interpreted as being generated by myocardial architecture with fiber parallel to the ultrasound direction. Currently, distribution or ratio of mid-circumferential fiber in the transmural left ventricular wall has not been elucidated. Hereafter, evaluation by echocardiography using anisotropic dropout may lead to new findings.

In this study, either echocardiography or histology is confined to 2-dimension, although myocardial fiber is structured 3-dimensionally, which is a point at issue. Magnetic resonance diffusion tensor imaging can provide for reconstruction of precise myocardial architecture within postmortem hearts[13]. A more accurate ultrasound orientation relative to the local fiber direction may be possible with such a new imaging modality.

In conclusion, the study demonstrated anisotropic characteristics in normal canine left ventricular

2-dimensional echograms with one-to-one histological validation. The acoustic dropout depended on the near parallel ultrasound orientation in respect to the local fiber direction.

Acknowledgments

We appreciate the initial participation of Michi Baba, the technical support of Noboru Ando, and temporarily providing an echocardiograph by Medical Teknika (Soka, Japan).

References

1. Mottley JG, Miller JG. Anisotropy of the ultrasonic backscatter of myocardial tissue: I. Theory and measurements in vitro. J Acoust Soc Am 1988;83:755-761.
2. Madaras EI, Perez J, Sobel BE, et al. Anisotropy of the ultrasonic backscatter of myocardial tissue: II. Measurements in vivo. J Acoust Soc Am 1988;83:762-769.
3. Mottley JG, Miller JG. Anisotropy of the ultrasonic attenuation in soft tissues: measurements in vitro. J Acoust Soc Am 1990;88:1203-1210.
4. Wickline SA, Verdonk ED, Miller JG. Three-dimensional characterization of human ventricular myofiber architecture by ultrasonic backscatter. J Clin Invest 1991;88:438-446.
5. Wickline SA, Verdonk ED, Wong AK, et al. Structural remodeling of human myocardial tissue after infarction. Quantification with ultrasonic backscatter. Circulation 1992;85:259-268.
6. Wong AK, Verdonk ED, Hoffmeister BK, et al. Detection of unique transmural architecture of human idiopathic cardiomyopathy by ultrasonic tissue characterization. Circulation 1992;86:1108-1115.
7. Verdonk ED, Hoffmeister BK, Wickline SA, et al. Anisotropy of the slope of ultrasonic attenuation in formalin fixed human myocardium. J Acoust Soc Am 1996;99:3837-3843.
8. Streeter DD, Jr., Spotnitz HM, Patel DP, et al. Fiber orientation in the canine left ventricle during diastole and systole. Circ Res 1969;24:339-347.
9. Anderson RH, Becker AE. The orientation of fibres within the ventricular mass. Cardiac anatomy: an integrated text and colour atlas. London: Gower Medical Publishing, 1980:5.14-5.26.
10. Aygen M, Popp RL. Influence of the orientation of myocardial fibers on echocardiographic images. Am J Cardiol 1987;60:147-152.
11. Holland MR, Wilkenshoff UM, Finch-Johnston AE, et al. Effects of myocardial fiber orientation in echocardiography: quantitative measurements and computer simulation of the regional dependence of backscattered ultrasound in the parasternal short-axis view. J Am Soc Echocardiogr 1998;11:929-937.
12. Sosnovik DE, Baldwin SL, Lewis SH, et al. Transmural variation of myocardial attenuation measured with a clinical imager. Ultrasound Med Biol 2001;27:1643-1650.
13. Schmid P, Jaermann T, Boesiger P, et al. Ventricular myocardial architecture as visualized in postmortem swine hearts using magnetic resonance diffusion tensor imaging. Eur J Cardiothorac Surg 2005;27:468-474.

Schizophrenia Bulletin vol. 36 no. 3 pp. 642–647, 2010
doi:10.1093/schbul/sbn132
Advance Access publication on October 16, 2008

Functional Deficits in the Extrastriate Body Area During Observation of Sports-Related Actions in Schizophrenia

Hidehiko Takahashi[1–3], Motoichiro Kato[4], Takeshi Sassa[5], Tomohisa Shibuya[5,6], Michihiko Koeda[7], Noriaki Yahata[8], Masato Matsuura[3], Kunihiko Asai[5], Tetsuya Suhara[2], and Yoshiro Okubo[7]

[2]Department of Molecular Neuroimaging, Molecular Imaging Center, National Institute of Radiological Sciences, 9-1, 4-chome, Anagawa,Inage-ku, Chiba 263-8555, Japan; [3]Department of Life Sciences and Bio-informatics, Graduate School of Health Sciences, Tokyo Medical and Dental University, 1-5-45 Yushima Bunkyo-ku, Tokyo 113-8549, Japan; [4]Department of Neuropsychiatry, Keio University School of Medicine, 35 Shinanomachi, Shinjuku-ku, Tokyo 160-8582, Japan; [5]Department of Psychiatry, Asai Hospital, 38-1 Katoku Togane 283-8650, Japan; [6]Department of Human Sciences, Toyo Gakuen University, 1-26-3, Hongo, Bunkyo-ku, Tokyo 113-0033, Japan; [7]Department of Neuropsychiatry and [8]Department of Pharamacology, Nippon Medical School, 1-1-5, Sendagi, Bunkyo-ku, Tokyo 113-8603, Japan

Exercise and sports are increasingly being implemented in the management of schizophrenia. The process of action perception is as important as that of motor execution for learning and acquiring new skills. Recent studies have suggested that body-selective extrastriate body area (EBA) in the posterior temporal-occipital cortex is involved not only in static visual perception of body parts but also in the planning, imagination, and execution of actions. However, functional abnormality of the EBA in schizophrenia has yet to be investigated. Using functional magnetic resonance imaging (fMRI) with a task designed to activate the EBA by sports-related actions, we aimed to elucidate functional abnormality of the EBA during observation of sports-related actions in patients with schizophrenia. Twelve schizophrenia patients and 12 age-sex–matched control participants participated in the study. Using sports-related motions as visual stimuli, we examined brain activations during observation of context-congruent actions relative to context-incongruent actions by fMRI. Compared with controls, the patients with schizophrenia demonstrated diminished activation in the EBA during observation of sports-related context-congruent actions. Furthermore, the EBA activation in patients was negatively correlated with the severity of negative and general psychopathology symptoms measured by the Positive and Negative Syndrome Scale. Dysfunction of the EBA might reflect a difficulty in representing dynamic aspects of human actions and possibly lead to impairments of simulation, learning, and execution of actions in schizophrenia.

Key words: body/extrastriate body area/schizophrenia/sports/exercise/fMRI

Introduction

With the introduction of atypical antipsychotics, awareness of these comorbid metabolic disturbances in schizophrenia has become considerably increased among many health care professionals and patients.[1] For the management of comorbid metabolic disturbances, exercise is one of the most acknowledged interventions.[2] At the same time, exercise and sports have been recognized as having a positive impact on the treatment and rehabilitation of schizophrenia.[3] However, individuals living with schizophrenia are less physically active than the general population.[4,5] Moreover, they generally show psychomotor poverty and clumsiness[6] and have an impairment of motor skill learning,[7,8] which have been suggested to be linked to a dysfunctional motor execution system including the striatum-frontal-cerebellum.[9,10]

It is widely documented in psychological and neurocognitive studies that the systems that mediate action perception, imitation, planning, and execution overlap and interact with each other.[11,12] These studies have supported the view that when we observe others' actions, observed action is automatically simulated and matched with internal motor representation and could even be imitated unconsciously (Chameleon effect).[12,13] These externally triggered motor representations are then used to understand, learn, and reproduce the observed behavior.[14] Therefore, for learning and acquiring new skills, the process of action perception is as important as that of motor execution.

Passive viewing of biological motions has been known to activate the superior temporal sulcus (STS),[15] and the STS has been suggested to have a more extended function in social cognition such as detecting intention of

[1]To whom correspondence should be addressed; tel: +81-43-206-3251, fax: +81-43-253-0396, e-mail: hidehiko@nirs.go.jp.

others.[16,17] Kim et al[18] reported that schizophrenia patients were impaired in the perception of biological motion, and they predicted that impaired biological motion processing arises from functional deficit in the STS. Although the STS is a central node of processing biological motion, passive viewing of biological motion has consistently activated the posterior temporal-occipital cortex including the body-selective extrastriate body area (EBA)[19] in close proximity to the STS.[20] Originally, the EBA was identified as an area that responds selectively to static human bodies and body parts.[19] In biological motion tasks, low-level visual stimuli such as random moving dots have been used as control task, which make it difficult to clarify whether the EBA is only involved in body-sensitive early visual processing or is participant as a part of a system for inferring the action and intention of others like the STS. However, recent studies have suggested an extended role for the EBA, involving not only static visual perception of body parts but also the planning, imagination, and execution of actions.[21,22] In addition, we have shown that sports-related context-congruent actions produced greater activation in the EBA, along with the STS, than context-incongruent actions.[23] Compared with frontal or limbic areas, the posterior temporal-occipital or temporal-parietal cortex has received relatively little attention in the field of schizophrenia research,[24] and functional abnormality of the EBA in schizophrenia has yet to be investigated. We hypothesized that patients with schizophrenia would show diminished activation in the EBA, along with the STS, in response to sports-related context-congruent actions.

Methods

Participants Twelve patients with schizophrenia (6 men and 6 women, mean age: 31.8 ± 7.2 [SD] years) were studied. Diagnoses were based on the Structured Clinical Interview for Diagnostic and Statistical Manual of Mental Disorders, Fourth Edition, Axis I Disorders. All patients were attending the day hospital unit of Asai Hospital. Exclusion criteria were current or past substance abuse and a history of alcohol-related problems, mood disorder, or organic brain disease. The mean illness duration was 9.8 ± 6.9 years. All patients received antipsychotics (mean chlorpromazine equivalent daily dosage = 641.6 ± 471.2 mg).[25,26] Clinical symptoms were assessed by the Positive and Negative Syndrome Scale (PANSS) for schizophrenia.[27] Mean total scores of PANSS and subscale (positive scale, negative scale, and general psychopathology scale) were 69.8 ± 13.6, 14.3 ± 4.0, 19.7 ± 4.7, and 35.8 ± 6.4, respectively. The ratings were reviewed by trained senior psychiatrists, H.T. and T.S., after the patient interviews, and disagreements were resolved by consensus; consensus ratings were used in this study. Twelve age-sex–matched normal controls (6 men and 6 women, mean age 29.4 ± 4.5 years) were recruited from the surrounding community. The candidates were carefully screened, and standardized interviews were conducted by H.T. and T.S.. They did not meet criteria for any psychiatric disorders. None of the controls were taking alcohol or medication at the time, nor did they have a history of psychiatric disorder, significant physical illness, neurological disorder, or alcohol or drug dependence. All subjects were right-handed, and they all underwent a magnetic resonance imaging (MRI) to rule out cerebral anatomic abnormalities. All subjects had achieved an educational level of high school or higher. All of them had the experience of playing basketball in elementary school or junior high school, but they had little opportunity, if any, to play basketball thereafter. After complete explanation of the study, written informed consent was obtained from all participants, and the study was approved by the Ethics Committee of Asai Hospital.

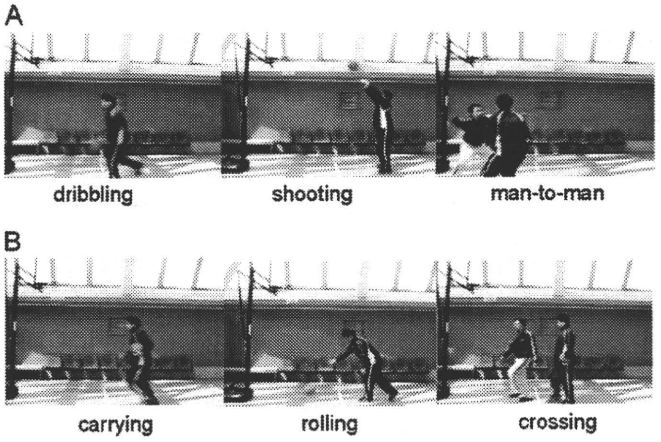

Fig. 1. Sample of Still Frames From Video Clips. A, Basketball-related motions; B, basketball-unrelated motions.

Materials

We employed the same visual stimuli as in the previous report where healthy volunteers were studied. The stimuli were designed to activate the EBA by sports-related actions.[23] Two types of video clips were provided (basketball-related motions [BRM] and basketball-unrelated motions [BUM]). Examples of the video clips are shown in figure 1. BRM consisted of 3 types of scenes (player shooting a free throw, player dribbling, 2 players performing man-to-man defense/offense). BUM also consisted of 3 types of scenes (player rolling a basketball, player carrying a basketball, and one person crossing in front of another without interaction). In order to make BRM and BUM as similar as possible, all players in the video clips performed in front of a basket hoop on a basketball court, and the number of persons, objects, motion direction, and speed were matched, ie, rolling a basketball, carrying a basketball, and crossing in front of another without interaction corresponded to shooting a free throw, dribbling, and man-to-man defense,

respectively. The video clips were projected via computer onto a screen mounted on a head coil. The subjects were instructed to pay attention to the video clips and to press a selection button with the right index finger when they watched the free throw scene and the basketball-rolling scene, indicating that they had paid attention to them. The experimental design consisted of 5 blocks for each of the 2 conditions (BRM and BUM) interleaved with 20-second rest periods. During the rest condition, participants viewed a crosshair pattern projected to the center of the screen. In the BRM and BUM 24-second blocks, 3 scenes were presented twice for 4 seconds each.

Image Acquisition

Images were acquired with a 1.5-T Signa system (General Electric, Milwaukee, WI). Functional images of 115 volumes were acquired with T2*-weighted gradient echo planar imaging sequences sensitive to blood oxygenation level–dependent contrast. Each volume consisted of 40 transaxial contiguous slices with a slice thickness of 3 mm to cover almost the whole brain (flip angle, 90°; echo time (TE), 50 ms; repetition time (TR), 4 sec; matrix, 64 × 64; field of view, 24 × 24 cm). High-resolution, T1-weighted anatomic images were acquired for anatomic comparison (124 contiguous axial slices; 3D Spoiled-Grass sequence; slice thickness, 1.5 mm; TE, 9 ms; TR, 22 ms; flip angle, 30°; matrix, 256 × 192; field of view, 25 × 25 cm).

Analysis of Functional Imaging Data

Data analysis was performed with SPM02 (Wellcome Department of Cognitive Neurology, London, UK). All volumes were realigned to the first volume of each session to correct for subject motion and were spatially normalized to the Montreal Neurological Institute template. Functional images were spatially smoothed with a 3D isotropic Gaussian kernel (full width at half maximum of 8 mm). Significant hemodynamic changes for each condition were examined using the general linear model with boxcar functions convolved with a hemodynamic response function. Statistical parametric maps for each contrast of the t statistic were calculated on a voxel-by-voxel basis.

To examine possible group differences in response to BUM (baseline), we conducted a 2-sample t test of BUM contrast. To assess the specific condition effect, we used the contrasts of BRM minus BUM. A random-effects model was implemented for group analysis. A 1-sample t test was applied to determine group activation for the contrasts of BRM minus BUM. Between-group comparison of BRM minus BUM contrast was performed with a 2-sample t test. We used SPM's small volume correction to correct for multiple testing in regions about which we had a priori hypotheses. These a priori volumes of interest (VOIs) included the EBA (inferior temporal cortex) and STS (superior temporal cortex). VOIs were defined by standardized VOI templates implemented in brain atlas software.[28] Significant differences surviving this correction at $P < .05$ were determined as were activations outside regions of interest surviving a threshold of $P < .001$, uncorrected, with an extent threshold of 10 contiguous voxels.

We conducted regression analyses to demonstrate a link between regional brain activities with the patients' demographics. Using the demographic data (age, duration of illness, chlorpromazine equivalent daily dosage, and PANSS scores) for each subject as covariates, regression analyses with the BRM minus BUM contrasts and the covariates were performed at the second level. The same threshold as used in the between-group comparison was applied. To confine the regions where significant group differences were observed, we created masks of group differences of the BRM minus BUM contrast from the 2-sample t test (threshold at $P < .05$, uncorrected), and these masks were applied inclusively. Using the effect sizes, representing the percent signal changes, of the BRM minus BUM contrasts at the peak coordinates uncovered in the regression analyses, we plotted the functional MRI (fMRI) signal changes and PANSS scores.

Results

Behavioral Data

All patients and controls paid attention to the video clips and pressed the button appropriately (accuracy was virtually 100%).

fMRI Results

In the control group, BRM minus BUM condition produced activations in the bilateral posterior temporal-occipital cortex including the bilateral EBA ($x = 58$, $y = -60$, $z = 2$; $t = 4.86$), middle temporal ($x = 54$, $y = -66$, $z = -12$; $t = 8.38$), right STS ($x = 56$, $y = -22$, $z = -2$; $t = 6.58$), bilateral premotor cortex ($x = -48$, $y = -4$, $z = 40$; $t = 4.94$), and bilateral inferior parietal lobules ($x = -34$, $y = -50$, $z = 54$; $t = 7.25$) (coordinates and t score refer to the peak of each brain region). In the patient group, BRM minus BUM condition produced activations in the left lingual gyrus ($x = -6$, $y = 92$, $z = 0$; $t = 6.52$), right prefrontal cortex ($x = 36$, $y = 52$, $z = 14$; $t = 5.66$), and right premotor cortex ($x = 36$, $y = -2$, $z = 54$; $t = 4.52$).

A 2-sample t test revealed no significant differences (threshold at $P < .001$, uncorrected) in the activations by BUM between controls and patients. Group comparison of the BRM minus BUM contrast showed that patients demonstrated significantly less activation in the bilateral EBA, bilateral parahippocampal gyrus, right STS, right temporal pole, right lingual gyrus, and globus pallidus (table 1 and figure 2). The activations in a priori regions (EBA and STS) survived a threshold of $P < .05$

Table 1. Regions showing diminished activation in response to BRM-BUM condition in 12 patients with schizophrenia compared with 12 controls

Brain regions	R/L	MNI coordinates			BA	t value	voxels
		x	y	z			
EBA (MTG)*	L	−40	−60	−4	37	5.37	106
EBA (MTG)*	R	52	−68	6	37	5.08	74
STS (STG)*	R	54	−22	0	21, 22	6.61	100
Temporal pole (STG)	R	40	10	−28	38	4.04	27
Parahippocampal gyrus	R	26	−26	−20	35	5.92	111
Parahippocampal gyrus	R	18	−38	−4	30	5.12	25
Parahippocampal gyrus	L	−28	−44	−6	19, 37	4.08	48
Lingual gyrus	R	6	−92	−10	17	4.28	21
Globus pallidus	R	16	−10	−2		4.12	21

Coordinates and t value refer to the peak of each brain region. MNI, Montreal Neurological Institute; BA, Brodmann area; L, left; R, right; MTG, middle temporal gyrus; STG, superior temporal gyrus BRM, basketball-related motions; BOM, basketball-unrelated motions; EBA, extrastriate body area; STS, superior temporal sulcus. All values, $P < .001$, uncorrected. *$P < .05$, corrected for multiple comparisons across a small volume of interest.

corrected for multiple comparisons across a small VOI. No significantly greater activation was identified in patients in the group comparison of the BRM minus BUM contrast.

Regression analysis revealed negative linear correlations between the negative scale score of PANSS and the degree of activation in the left EBA (x = −58, y = −58, z = −6; t = 7.01) in BRM minus BUM contrast (figure 3). Scores of the general psychopathology scale were also negatively correlated with the degree of activation in the left EBA (x = −58, y = −56, z = −6; t = 5.81) (figure 3). These correlations in a priori regions (EBA) survived a threshold of $P < .05$ corrected for multiple comparisons across a small VOI. There was no correlation between the positive scale score and regional brain activation. Regression analysis revealed that none of age, duration of illness, or chlorpromazine equivalent daily dosage had a relation with regional brain activation.

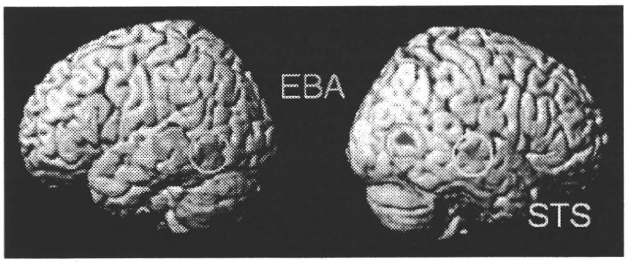

Fig. 2. Images Showing the Brain Area of **D**iminished Activations in Response to Basketball-Related Motions (BRM) Relative to Basketball-Unrelated Motions (BUM) Condition in 12 Patients With Schizophrenia Compared With 12 Normal Controls. **D**iminished activations in the bilateral extrastriate body area (EBA), right superior temporal sulcus (STS), and right temporal pole are shown.

Discussion

This study demonstrated that patients with schizophrenia showed diminished brain activations during observation of context-congruent actions in the EBA, along with the STS. The coordinates of the EBA were in good agreement with the previous literature (reviewed in Arzy et al[29]). The lesser activation of the STS in the patients was fairly predicted because previous psychological study has shown the impairment of biological motion perception in schizophrenia, which has been thought to be attributable to dysfunction of the STS.[18] The STS is located at a convergence zone for multimodal signals including limbic information,[30] and it has been suggested to be involved not only in the perception of biological motion but also in a more extended function of social cognition such as understating others' intention.[16,17] Dysfunctional STS might contribute to a difficulty in understanding intentional actions and behavior of agents in schizophrenia.[31]

The novel finding in this study was that the patients showed diminished EBA activation in response to context-congruent actions despite the fact that the patients comprehended explicit information of body movement (and basketball rules) similar to controls. This implies that the patients might not have processed implicit information carried by body movements as much as controls, but it is very difficult to quantify such implicit information and complex EBA function in a limited MRI environment and in a limited time period. Interestingly, PANSS score, instead of performance during fMRI scans, was directly linked to EBA activation in patients. That is, the less EBA activation was, the more severe the symptoms (negative and general psychopathology) in the patients were. The EBA was first identified as an area that responds selectively to static human bodies.[19] Recent

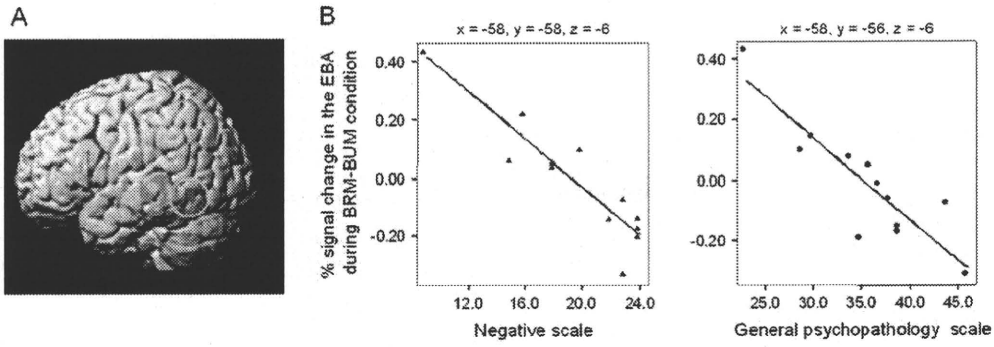

Fig. 3. Negative Correlations Between Positive and Negative Syndrome Scale (PANSS) Scores and the Degree of Activation in the Extrastriate Body area (EBA). A, Images showing negative correlation between negative scale scores and the degree of activation in the left EBA in basketball-related motions-basketball-unrelated motions (BRM-BUM) contrast. Scores of general psychopathology scale were also negatively correlated with the degree of activation in the left EBA in BRM-BUM contrast, yielding images identical to A. B, Plots and regression lines of negative correlations between PANSS scores and the degree of activation in the left EBA. The degrees of activations in the EBA were negatively correlated with the scores of negative scale ($r = -0.91$, $df = 10$; $P < .001$) and general psychopathology scale ($r = -0.88$, $df = 10$; $P < .001$).

studies have suggested that the EBA is also directly involved in representing the dynamic aspects of human motions as part of a system for inferring the intention of others.[32] Jackson et al[22] reported that, compared with observation of actions, EBA activation was enhanced during imitation. Furthermore, the motivation to act has been shown to modulate EBA activity.[33] These studies proposed an extended role for the EBA, involving the planning, execution, and imagination of actions. Our previous report that using the current task in healthy volunteers was in favor of this view,[23] suggesting that the EBA might contribute to the understanding of actions and intention of others through the mechanism of observed action being automatically represented and simulated.[14,32]

Empirical studies have shown that schizophrenia patients have difficulty in representing motor actions internally.[34,35] The diminished EBA activation in patients suggests that internal representation of the dynamic aspects of human motions is impaired. Motor representation is associated with understanding and rehearsing observed behavior.[14] In fact, recent studies demonstrated that motor representation is highly involved in skill learning and motor rehabilitation.[36,37] Consequently, the deficit in the EBA in schizophrenia could lead to difficulties in learning and reproducing new skills in addition to impairment in understanding others' actions.

The present study has several limitations. First, we examined only patients with chronic schizophrenia with long-term antipsychotic medication because our primary interest was the possible role of sports participation/observation in the management of chronic schizophrenia and comorbid metabolic disturbances partly due to antipsychotic medication. Medication possibly affects neural activation, but regression analysis revealed that chlorpromazine equivalent daily dosage has no relation with regional brain activation, and expression of dopamine D2 receptors in the posterior temporal-occipital cortex is extremely low.[38] Second, our task was not a behaviorally/cognitively demanding task leading to lack of dispersion in behavioral data (100% accuracy for both control and patient groups). Using a behaviorally/cognitively demanding task would require us to include only patients with psychiatric symptoms and cognitive impairments mild enough to undergo the imaging procedure and comply with the demanding task. However, the target patients of rehabilitation and management of comorbid metabolic disturbances in a day hospital have considerable behavioral and cognitive disturbances, which make it difficult to obtain reliable self-reported data of complex and subtle functions. Therefore, we employed the current task, aiming to examine patients with chronic schizophrenia in a real-world setting. From these limitations, it must be emphasized that any generalization of our findings to patients with first episode or nondeficit patients needs to be approached with caution.

In conclusion, chronic schizophrenia patients demonstrated diminished activation in the EBA in response to sports-related actions. Dysfunction of the EBA might reflect impairment of representation of dynamic aspects of human actions and might lead to impairments in simulation, learning, and execution of actions in schizophrenia. Furthermore, these impairments might lead to difficulty in understanding others' actions, interpersonal communication, body awareness, and overall physical activity manifested as negative symptoms and general psychopathology symptoms. The results of this study seem to have some important clinical implications for the management of chronic schizophrenia and merit further investigation in terms of the role of sports participation/observation in the rehabilitation for chronic schizophrenia and their effects on EBA function.

Funding

Japanese Ministry of Health, Labor and Welfare (Health and Labor Sciences Research Grant for Research on

Psychiatric and Neurological Diseases and Mental Health H20-KOKORO-025).

Acknowledgments

Mieko Mori and Harumi Murayama and the staff of the day hospital unit of Asai Hospital are gratefully acknowledged for nursing care and assistance with subject recruitment.

References

1. Henderson DC. Diabetes mellitus and other metabolic disturbances induced by atypical antipsychotic agents. Curr Diab Rep. 2002;2:135–140.
2. Menza M, Vreeland B, Minsky S, Gara M, Radler DR, Sakowitz M. Managing atypical antipsychotic-associated weight gain: 12-month data on a multimodal weight control program. J Clin Psychiatry. 2004;65:471–477.
3. Langle G, Siemssen G, Hornberger S. Role of sports in treatment and rehabilitation of schizophrenic patients. Rehabilitation (Stuttg). 2000;39:276–282.
4. Daumit GL, Goldberg RW, Anthony C, et al. Physical activity patterns in adults with severe mental illness. J Nerv Ment Dis. 2005;193:641–646.
5. Faulkner G, Cohn T, Remington G. Validation of a physical activity assessment tool for individuals with schizophrenia. Schizophr Res. 2006;82:225–231.
6. Boks MP, Russo S, Knegtering R, van den Bosch RJ. The specificity of neurological signs in schizophrenia: a review. Schizophr Res. 2000;43:109–116.
7. Kodama S, Fukuzako H, Fukuzako T, et al. Aberrant brain activation following motor skill learning in schizophrenic patients as shown by functional magnetic resonance imaging. Psychol Med. 2001;31:1079–1088.
8. Weickert TW, Terrazas A, Bigelow LB, et al. Habit and skill learning in schizophrenia: evidence of normal striatal processing with abnormal cortical input. Learn Mem. 2002;9:430–442.
9. Alexander GE, DeLong MR, Strick PL. Parallel organization of functionally segregated circuits linking basal ganglia and cortex. Annu Rev Neurosci. 1986;9:357–381.
10. Andreasen NC. A unitary model of schizophrenia: Bleuler's "fragmented phrene" as schizencephaly. Arch Gen Psychiatry. 1999;56:781–787.
11. Grezes J, Decety J. Functional anatomy of execution, mental simulation, observation, and verb generation of actions: a meta-analysis. Hum Brain Mapp. 2001;12:1–19.
12. Iacoboni M, Dapretto M. The mirror neuron system and the consequences of its dysfunction. Nat Rev Neurosci. 2006; 7:942–951.
13. Chartrand TL, Bargh JA. The chameleon effect: the perception-behavior link and social interaction. J Pers Soc Psychol. 1999;76:893–910.
14. Brass M, Heyes C. Imitation: is cognitive neuroscience solving the correspondence problem? Trends Cogn Sci. 2005; 9:489–495.
15. Allison T, Puce A, McCarthy G. Social perception from visual cues: role of the STS region. Trends Cogn Sci. 2000;4:267–278.
16. Frith U, Frith CD. Development and neurophysiology of mentalizing. Philos Trans R Soc Lond B Biol Sci. 2003;358:459–473.
17. Gallagher HL, Frith CD. Functional imaging of 'theory of mind'. Trends Cogn Sci. 2003;7:77–83.
18. Kim J, Doop ML, Blake R, Park S. Impaired visual recognition of biological motion in schizophrenia. Schizophr Res. 2005;77:299–307.
19. Downing PE, Jiang Y, Shuman M, Kanwisher N. A cortical area selective for visual processing of the human body. Science. 2001;293:2470–2473.
20. Peelen MV, Wiggett AJ, Downing PE. Patterns of fMRI activity dissociate overlapping functional brain areas that respond to biological motion. Neuron. 2006;49:815–822.
21. Astafiev SV, Stanley CM, Shulman GL, Corbetta M. Extrastriate body area in human occipital cortex responds to the performance of motor actions. Nat Neurosci. 2004;7:542–548.
22. Jackson PL, Meltzoff AN, Decety J. Neural circuits involved in imitation and perspective-taking. Neuroimage. 2006;31:429–439.
23. Takahashi H, Shibuya T, Kato M, et al. Enhanced activation in the extrastriate body area by goal-directed actions. Psychiatry Clin Neurosci. 2008;62:214–219.
24. Torrey EF. Schizophrenia and the inferior parietal lobule. Schizophr Res. 2007;97:215–225.
25. Rey MJ, Schulz P, Costa C, Dick P, Tissot R. Guidelines for the dosage of neuroleptics. I: Chlorpromazine equivalents of orally administered neuroleptics. Int Clin Psychopharmacol. 1989;4:95–104.
26. Rijcken CA, Monster TB, Brouwers JR, de Jong-van den Berg LT. Chlorpromazine equivalents versus defined daily doses: how to compare antipsychotic drug doses? J Clin Psychopharmacol. 2003;23:657–659.
27. Kay SR, Fiszbein A, Opler LA. The positive and negative syndrome scale (PANSS) for schizophrenia. Schizophr Bull. 1987;13:261–276.
28. Maldjian JA, Laurienti PJ, Kraft RA, Burdette JH. An automated method for neuroanatomic and cytoarchitectonic atlas-based interrogation of fMRI data sets. Neuroimage. 2003; 19:1233–1239.
29. Arzy S, Thut G, Mohr C, Michel CM, Blanke O. Neural basis of embodiment: distinct contributions of temporoparietal junction and extrastriate body area. J Neurosci. 2006;26:8074–8081.
30. Puce A, Perrett D. Electrophysiology and brain imaging of biological motion. Philos Trans R Soc Lond B Biol Sci. 2003; 358:435–445.
31. Russell TA, Reynaud E, Herba C, Morris R, Corcoran R. Do you see what I see? Interpretations of intentional movement in schizophrenia. Schizophr Res. 2006;81:101–111.
32. Jeannerod M. Visual and action cues contribute to the self-other distinction. Nat Neurosci. 2004;7:422–423.
33. Cheng Y, Meltzoff AN, Decety J. Motivation modulates the activity of the human mirror-neuron system. Cereb Cortex. 2007;17:1979–1986.
34. Danckert J, Rossetti Y, d'Amato T, Dalery J, Saoud M. Exploring imagined movements in patients with schizophrenia. Neuroreport. 2002;13:605–609.
35. Maruff P, Wilson P, Currie J. Abnormalities of motor imagery associated with somatic passivity phenomena in schizophrenia. Schizophr Res. 2003;60:229–238.
36. Calvo-Merino B, Glaser DE, Grezes J, Passingham RE, Haggard P. Action observation and acquired motor skills: an FMRI study with expert dancers. Cereb Cortex. 2005;15:1243–1249.
37. Ertelt D, Small S, Solodkin A, et al. Action observation has a positive impact on rehabilitation of motor deficits after stroke. Neuroimage. 2007;36(Suppl. 2):T164–173.
38. Okubo Y, Olsson H, Ito H, et al. PET mapping of extrastriatal D2-like dopamine receptors in the human brain using an anatomic standardization technique and [11C]FLB 457. Neuroimage. 1999;10:666–674.

Psychiatry and Clinical Neurosciences 2011; 65: 191–198 doi:10.1111/j.1440-1819.2011.02189.x

Regular Article

Functional magnetic resonance imaging study on the effects of acute single administration of paroxetine on motivation-related brain activity

Toshiyuki Marutani, MD,[1,2] Noriaki Yahata, PhD,[3,4] Yumiko Ikeda, MS,[3] Takehito Ito, PhD,[1] Manami Yamamoto, PhD,[1] Masato Matsuura, MD, PhD,[5] Eisuke Matsushima, MD, PhD,[2] Yoshiro Okubo, MD, PhD,[6] Hidenori Suzuki, MD, PhD[3] and Tetsuya Matsuda, PhD[1]*

[1]*Tamagawa University Brain Science Institute,* [2]*Section of Liaison Psychiatry & Palliative Medicine, Graduate School of Tokyo Medical & Dental University,* [3]*Department of Pharmacology, Nippon Medical School,* [4]*Department of Neuropsychiatry, Graduate School of Medicine, University of Tokyo,* [5]*Section of Biofunctional Informatics, Graduate School of Allied Health Sciences, Tokyo Medical and Dental University, and* [6]*Department of Neuropsychiatry, Nippon Medical School, Tokyo, Japan*

Aim: The aim of the present study was to investigate the effects of acute paroxetine administration on brain activity related to motivation.

Methods: Sixteen healthy subjects participated in a randomized, single-blind, no-drug/placebo-controlled, cross-over study. After administration of no drug, placebo or paroxetine (selective serotonin reuptake inhibitor; 20 mg), subjects underwent functional magnetic resonance imaging while performing a monetary incentive delay task. We analyzed the differences in brain activities of the reward anticipation/motor preparation period that are subject to motivational modulation. For this purpose, we subdivided the incentive trials on the basis of whether the reaction times (RT) were slower or faster than the subject's mean RT (slow RT and fast RT trials).

Results: No drug and placebo showed robust activation differences in the globus pallidus and putamen for the fast RT trials compared to the slow RT trials, whereas paroxetine showed none. Paroxetine showed significantly lower activations in the globus pallidus, insula, putamen and dorsolateral prefrontal cortex compared to no drug in the fast RT trials.

Conclusions: Paroxetine single acute administration diminished brain activity induced by motivation in healthy subjects. This may partially explain the increased lack of motivation seen in patients with relatively mild symptoms after taking a dose of paroxetine for the first time.

Key words: functional magnetic resonance imaging, motivation, paroxetine, reaction time, reward anticipation.

SELECTIVE SEROTONIN REUPTAKE inhibitors (SSRI) are first-line drugs for the treatment of major depressive disorder (MDD). MDD is characterized by disturbances in emotion, motivation and behavior in the presence of autonomic nervous symptoms.[1] A core symptom of MDD includes decreased motivation,[2,3] which SSRI sometimes rather aggravate in some patients.[4–6]

Motivational processing includes reward anticipation, motor preparation and related processes, including arousal and attention.[7,8] Several pharmacological functional magnetic resonance imaging (fMRI) studies have assessed the functions and/or mechanisms of SSRI related to motor, attention and reward. The effects of SSRI on motor function,[9,10] attention,[11] loss/no-loss comparison[12] and neural

Correspondence: Tetsuya Matsuda, PhD, Tamagawa University Brain Science Institute, 6-1-1, Tamagawa Gakuen, Machida, Tokyo 194-8610, Japan. Email: tetsuya@lab.tamagawa.ac.jp
Received 15 September 2010; revised 23 December 2010; accepted 23 December 2010.

processing of both rewarding and aversive stimuli[13] in healthy subjects have been studied by fMRI. McCabe reported that seven days of citalopram treatment diminished the brain activity induced by deliveries of rewards and aversive stimuli. They used primary rewards, chocolate taste and unpleasant strawberry taste as stimuli. Their conclusion indicated that the results could explain the experience of emotional blunting described by some patients during SSRI treatment.[13–15]

Decrease in motivation is also clinically observed after taking an initial dosing.[16] We have clinically observed some patients, especially patients with mild symptoms who reported decreased motivation after taking an initial dose of SSRI. Then, in the present study, we focused on the effects of an SSRI single acute administration on brain activity during motor preparation and reward anticipation, which are subject to motivational modulation. For this purpose, we used a monetary incentive delay (MID) task.[17] This task has been used in numerous reward-processing studies, and variations of the MID task have been used in a variety of other research.[18–20] Regardless of the details, the reward anticipation/motor preparation period and the subsequent button press during the task are essential. It is likely that the subject's motivations fluctuate over repeated trials of the MID task, and this is reflected in reaction time (RT). We expected that paroxetine would attenuate brain activity induced by motivation.

METHODS

Subjects

Sixteen healthy subjects participated in this study, but two were excluded because of an extremely low hit rate (less than 60%). Fourteen healthy subjects (eight men, mean age ± SD: 31 ± 3.8 years) were included in the final analysis. All subjects were native Japanese speakers and right-handed, as assessed by the Edinburgh Handedness Inventory. They filled out a questionnaire about their medical history and medications and were then interviewed by a medical staff member. They had no history of present or past psychiatric illnesses, neurological disorders, significant physical illnesses or head injuries, and no alcohol- or drug-related problems. They had not taken any types of medication for at least 1 day prior to scanning.

After a complete explanation of the study, including the possible side-effects of paroxetine, written informed consent was obtained from all the subjects and all the subject identifiers were removed. The protocol was approved by the local ethics committee.

Drug administration

We chose paroxetine as the SSRI for this study because it has the highest affinity for the human serotonin (5-HT) transporter among SSRI and other antidepressants according to radioligand binding assay studies[21–23] with a reported equilibrium dissociation constant (K_D) of 0.13 ± 0.01 nmol.

All subjects were examined after administration of paroxetine (S, 20 mg [minimally effective dose] paroxetine hydrochloride hydrate tablet), placebo (P, 12 mg lactobacillus bifidus tablet) or no drug (N) in a randomized, single-blind, no drug/placebo controlled, cross-over design. Three to 43 days (average 14.0 ± 13.7 days) passed between experiments. The order of drug administration was counterbalanced across subjects. The drug administration order consisted of six combinations (N-P-S, N-S-P, P-N-S, P-S-N, S-N-P, S-P-N) and we randomly assigned each combination to each subject.

The maximum drug concentration time (Tmax) of paroxetine 20 mg was reported to be 5.05 ± 1.22 h in healthy Japanese subjects.[24] Accordingly, placebo (P) and paroxetine (S) were given 5–5.5 h before initiating scanning to ensure maximum and stable plasma concentrations.

A previous positron emission tomography study suggests that 80% 5-HT transporter blockade is important for therapeutic effect of SSRI.[25] A single dosing of minimum therapeutic dose of an SSRI showed around 80% 5-HT transporter occupancy, which was almost the same as long-term dosing data.[26] Accordingly, a single dosing of paroxetine 20 mg of this study should have enough 5-HT transporter occupancy for therapeutic effect.

Reward task

Subjects performed an incentive task during functional scanning after a short pre-scanning training task. The task paradigm was an event-related design. The task was created with E-Prime 1.2 (Psychology Software Tools), which consisted of 98 7–8-s trials with 4-s inter-trial intervals (approx. 19 min. total). During each trial, subjects were shown one of three cue shapes (500 ms), a fixed crosshair during a variable delay (2500–3500 ms), and they responded with

a button press during the presentation of a gray square target (500 ms). They were then shown a fixed yellow crosshair (3000 ms) and this was followed by feedback (500 ms) notifying subjects if they had gained the points indicated by the cue, gained no points (= 0 point), or failed to press the button within 500 ms. The inter-trial interval was set to 4000 ms.

The cues signaled the possibility of no gain, 0 points ($n = 10$; denoted by a circle), 100 points ($n = 44$; denoted by a circle with one horizontal line) or 500 points ($n = 44$; denoted by a circle with three horizontal lines). There were three pseudorandom and predetermined orders of trials presented to subjects depending on experimental order, i.e. the combinations of medication and trial presentation order were counterbalanced.

Before scanning, subjects were instructed that the duration of target presentation was fixed to 500 ms but the button press limits differed from trial to trial. Fourteen 100-point cue and 500-point cue trials were predetermined to have a feedback of 0 points despite any efforts. In eight of these 28 trials, RT were not collected and were excluded from the analysis. The other trials required a fixed 500-ms time limit for the button press. If the subject did not respond in the appropriate interval, the message 'Press the button!' was displayed. We asked subjects to respond as quickly as possible to gain the maximum number of points, but the points earned were not reflected in the payment for participation in the study. Subjects were also asked to respond within the target presentation time even if the cue was a circle without line (potential 0 points). The total points earned were displayed at the end of the session.

During the original MID task,[17] RT were collected during the practice session so that the task difficulty level was set to achieve a success rate of 66%. However, we fixed the target duration to 500 ms so that the hit rate would reflect subjects' efforts more accurately. We also performed more trials to compare the effects of differences of RT in incentive trials. To maintain cue incentives, predetermined trials of gain cued with non-gain feedback were intermixed. Subjects were not told of their running point totals to minimize possible confounding effects.

fMRI data acquisition

The fMRI scans were acquired with a 3T Siemens MAGNETOM Trio Tim system scanner (Siemens, Erlangen, Germany). A total of 575 functional images were taken with a T2*-weighted gradient echo planer imaging sequence (TE = 25 ms; TR = 2000 ms; FA = 90°; matrix 64 × 64; FOV 192 × 192 cm) sensitive to the blood oxygenation level dependent (BOLD) contrast. Whole brain coverage was obtained with 34 axial slices (thickness 4 mm; in-plane resolution 3 × 3 mm).

Behavioral data analysis

For each drug condition for each subject, the mean RT to the target was calculated. Trials in which subjects did not press the button within the time limit were excluded from this calculation. Since the goal of this study was to investigate motivational motor preparation, we divided the RT of the incentive trials (100 and 500 points) on the basis of whether the RT were slower or faster than the subject's mean RT (RTslow and RTfast). For the purpose of this analysis, the 100- and 500-point trials were pooled to increase the sample set; there were no significant differences in hit rate or proportion of successful button presses among drug conditions for the different point trials. The mean RT of the slow RT and the fast RT trials were calculated, and these data were entered into a 3 (drug: non-drug, placebo, and paroxetine) × 2 (RT: slow and fast)-repeated-measures ANOVA using SPSS 16.0 J (SPSS Japan, Tokyo, Japan). The level of significance was set at 0.05.

fMRI data analysis

Image pre-processing and data analysis were performed with the statistical parametric mapping software package, SPM5 (Wellcome Department of Imaging Neuroscience, London, UK) running MATLAB 2007a (Mathworks, Natick, MA, USA). During pre-processing, the echo planer images were corrected for sequential slice timing, and all images were realigned to the first image to adjust for possible head movements. The realigned images were then spatially normalized to a standard Montreal Neurological Institute (MNI) template.[27] After normalization, all scans had a resolution of $2 \times 2 \times 2$ mm^3. Functional images were spatially smoothed with a 3-D isotropic Gaussian kernel (full width at half maximum of 8 mm). Low-frequency noise was removed by applying a high-pass filter (cut-off period = 192 s) and the default correction for AR1 auto correlation was performed for the fMRI time series at each voxel. A temporal smoothing function

was applied to the fMRI time series to enhance the temporal signal-to-noise ratio. Significant hemodynamic changes for each condition were examined using the general linear model with boxcar functions convoluted with a hemodynamic response function. Statistical parametric maps for each contrast of t-statistic were calculated on a voxel-by-voxel basis.

We then assessed the RT effect for each drug condition and the drug effect for the slow or fast RT during reward anticipation. We divided the trials into slow and fast RT trials, and we created the t-contrasts for the anticipation period between the offset of cue presentation and the onset of target presentation for the three different drug conditions in single-subject analysis (Nslow, Nfast, Pslow, Pfast, Sslow, Sfast).

A random effects analysis was performed to examine for population-wide effects. First, we used a 3 (medication: no drug, placebo and paroxetine) × 2 (RT: fast and slow) full factorial design to investigate brain activation between the different RT trials under each drug condition. There were significant activations for Nfast > Nslow in basal ganglia and primary motor cortex of which evident correlations have been revealed with reward anticipation[17,18,28,29] and motor preparation,[30] whereas activations for Pfast > Pslow and Sfast > Sslow were almost none. Then, to focus on regional activations in the reward anticipation and motor preparation-related areas in placebo and paroxetine, after paired *t*-tests were applied to Nfast > Nslow at the $P < 0.001$ level, uncorrected, with a voxel threshold of k = 10, we proceeded to a region-of-interest (ROI) analysis.

RESULTS

Behavioral data

The average hit rate of 90 trials was 92.9 ± 5.5%, 95.5 ± 4.2%, and 92.8 ± 6.7% for no drug, placebo, and paroxetine, respectively.

The average RT of all the trials and of the incentive (100 and 500 points) trials were 297.42 ± 38.69 ms and 294.02 ± 42.66 ms, 294.03 ± 40.31 ms and 290.45 ± 46.69 ms, 299.77 ± 38.96 ms and 298.08 ± 44.72 ms, under no drug, placebo and paroxetine conditions, respectively. There were no significant differences among three drug conditions.

Then we subdivided the RT of each incentive trial based on their relationship to the subject's mean RT, and the mean RT of each group, RTslow and RTfast, were compared for each drug treatment group.

A 3 (drug: non-drug, placebo, and paroxetine) × 2 (RT: slow and fast)-repeated-measures ANOVA revealed an effect of RT, $F_{1,13} = 398.73$, $P < 0.001$. Post hoc analyses with Bonferroni correction showed significant differences between RTslow and RTfast for each drug condition. RTslow and RTfast were 329.70 ± 27.04 ms and 258.34 ± 19.12 ms, 327.64 ± 31.61 ms and 253.25 ± 24.36 ms, 334.74 ± 30.04 ms and 261.43 ± 20.26 ms under no drug, placebo and paroxetine conditions, respectively. However, no significant differences were detected in the same RT (slow or fast) group among the different drug conditions.

fMRI data

The significantly activated areas for Nfast > Nslow were left primary motor cortex (T = 8.50), left globus pallidus (GP) (T = 5.95), right GP (T = 5.14), left dorsolateral prefrontal cortex (DLPFC) (T = 5.57), left transverse temporal gyrus (T = 5.26), right transverse temporal gyrus (T = 5.26), left thalamus (T = 4.87), right thalamus (T = 3.53), left insula (T = 4.71), right insula (T = 4.69), left putamen (T = 4.41), right putamen (T = 4.57), vermis (T = 4.50), right nucleus accumbens (NAcc) (T = 4.49) and left caudate (T = 4.27).

To investigate motivation-related areas under placebo and paroxetine conditions, we then performed a ROI analysis for the peak voxel of the regions significantly activated in Nfast > Nslow whole brain *t*-test. The ROI were selected based on previous fMRI studies of reward anticipation; GP,[28] insula,[27,29] putamen,[17,18,29] NAcc,[17] caudate,[29] DLPFC[31] and motor preparation; primary motor cortex.[30] The MNI coordinates [x y z] of ROI were left GP [−24 −10 0], right GP [20 −10 0], left insula [−38 −14 10], right insula [40 2 8], left putamen [−22 8 −2], right putamen [28 4 8], right NAcc [10 10 −14], left caudate [−6 12 4], left DLPFC [−36 32 26] and left primary motor cortex [−32 −22 54]. We collected beta values of each ROI and entered the data into 3 (drug conditions: N, P, S) × 2 (RT: slow, fast)-repeated-measures ANOVA using SPSS 16.0J. The level of significance was set at 0.05.

This ROI analysis using an ANOVA with repeated measures revealed a significant interaction between drug and RT in left insula ($F_{2,26} = 4.406$, $P = 0.022$), right insula ($F_{2,26} = 5.379$, $P = 0.011$), right NAcc ($F_{2,26} = 3.387$, $P = 0.049$), left primary motor cortex ($F_{2,26} = 4.016$, $P = 0.030$), a significant drug effect in

right insula ($F_{1,13} = 6.948$, $P = 0.021$) and left primary motor cortex ($F_{2,26} = 7.894$, $P = 0.002$), a significant RT effect in left GP ($F_{1,13} = 1.573$, $P < 0.0001$), right GP ($F_{1,13} = 37.957$, $P < 0.0001$), right insula ($F_{1,13} = 6.948$, $P = 0.021$), left putamen ($F_{1,13} = 45.757$, $P < 0.0001$), right putamen ($F_{1,13} = 13.968$, $P = 0.002$), right NAcc ($F_{1,13} = 5.755$ $P = 0.032$), left caudate ($F_{1,13} = 10.553$, $P = 0.006$), left DLPFC ($F_{1,13} = 10.568$, $P = 0.006$) and left primary motor cortex ($F_{1,13} = 38.179$, $P < 0.0001$).

Post hoc analysis with Bonferroni correction showed there were significant differences between paroxetine and placebo in only the left primary motor cortex, Pslow and Sslow ($P = 0.003$), Pfast and Sfast ($P = 0.008$), in which the activations were greater under placebo treatment (Fig. 1j). In the absence of drug or placebo treatment, the fast RT trials (Nfast) showed significantly higher activation than the fast RT trials of paroxetine condition (Sfast) in left GP ($P = 0.023$), left insula ($P = 0.008$), right insula ($P = 0.007$), right putamen ($P = 0.008$), left DLPFC ($P = 0.022$) and left primary motor cortex ($P = 0.003$) (Fig. 1a,c,d,f,i,j), which was not shown in comparison between the slow RT trials. There were no significant differences between placebo and no drug in any of the ROI.

Considering the way the ROI were defined, it was natural that there were significant differences between Nslow and Nfast in all the ROI. In paroxetine conditions, Sfast was significantly more activated than Sslow in only the left primary motor cortex (Fig. 1j). When subjects were given placebo, Pfast activation was greater than Pslow only in the left GP ($P = 0.045$), left putamen ($P = 0.007$) and left primary motor cortex ($P = 0.042$) (Fig. 1a,e,j).

DISCUSSION

Disturbances in motivation and motor activity are seen in MDD and these symptoms are sometimes exacerbated by SSRI in some patients. To investigate this paradoxical effect, we wish to use fMRI to monitor affected patients in response to drug therapy. However, as a first step, we studied normal subjects following a single dose of the SSRI paroxetine.

In this collection of normal subjects, there were no differences among the three drug conditions within each of the average RT of the whole, no incentive, incentive and subdivided RT trials. Thus, paroxetine administration did not affect subject behavior or performance globally. The average RT of no incentive and incentive trials showed no significance, which might be induced by the instruction for the subjects to press the button within the short duration of 500 ms even when the cue was no incentive.

Then, we investigated brain activations between the slow RT and the fast RT trials, which were behaviorally subdivided with significance, within treatment groups. The fast RT trials recruited greater activation in the GP, insula, putamen, NAcc, DLPFC, caudate and primary motor cortex than slow RT trials under no drug treatment. Under placebo conditions, the fast RT trials recruited greater activation in the GP, putamen and primary motor cortex. However, the paroxetine condition showed greater activations in the fast RT trials compared to the slow RT trials only in the primary motor cortex. These results indicated paroxetine desensitized RT influence on reward-anticipation-related brain activity, meanwhile no drug and placebo conditions reflected RT influence fully or partially in the reward-related areas.

In the next step, we looked into the activation differences in the same RT (slow or fast) group among the different drug conditions. Paroxetine significantly suppressed activation in the left GP, bilateral insula, right putamen and left DLPFC as reward-anticipation-related areas compared to no drug in the fast RT trials reflecting higher motivation, not in the slow RT trials reflecting lower motivation.

In the primary motor cortex, the activation under paroxetine administration was significantly weaker than no drug in the fast RT trials only, but weaker than placebo in both fast and slow RT trials. Besides, the fast RT trials were activated greater than the slow RT trials in all three drug conditions. Thus, the characteristics shown in the reward-related areas collapsed in the primary motor cortex, although paroxetine reduced activation compared to no drug and placebo in any case.

Taken together, paroxetine attenuated the brain activity in the reward-anticipation-related areas between the subdivided RT groups and compared to no drug in the more motivated fast RT trials. When anhedonia, one of the major symptoms of MDD, is considered as decreased motivation and sensitivity to rewarding experiences, our results suggest that a single dose of paroxetine may create a relatively anhedonic state in healthy subjects.